Iterative Solution Methods for Beam Angle and Fluence Map Optimization in Intensity Modulated Radiation Therapy Planning

Gino J. Lim[1], Jaewon Choi[1], and Radhe Mohan[2]

Abstract

We present computational approaches for optimizing beam angles and fluence maps in Intensity Modulated Radiation Therapy (IMRT) planning. We assume that the number of angles to be used for the treatment is given by the treatment planner. A mixed integer programming (MIP) model and a linear programming (LP) model are used to find an optimal set of beam angles and their corresponding fluence maps. The MIP model is solved using the branch-and-bound method while the LP model is solved using the interior point method. In order to reduce the computational burden for solving the optimization models, we introduce iterative beam angle elimination algorithms in which an insignificant beam angle is eliminated in each iteration. Other techniques are also explored including feasible set reduction for LP and data reduction. Experiments are made to show the computational advantage of the iterative methods for optimizing angles using real patient cases.

[1] Department of Industrial Engineering, University of Houston, 4800 Calhoun Road, Houston, TX 77204. Email: ginolim@uh.edu

[2] Department of Radiation Physics, University of Texas - MD Anderson Cancer Center, Houston, TX

1. Introduction

Cancer is the second leading cause of death in the United States [2], but it can be treated if it is diagnosed in its early stages. Several options are available for treatment: surgery, radiation therapy, chemotherapy, hormone therapy, or a combination of such methods. Thanks to significant advances in radiation treatment techniques, radiation therapy has become a popular non-invasive option by itself and in combination with other methods. Developing a safe radiation therapy plan is not an easy task because tumors are typically surrounded by healthy organs. Even for a highly skilled expert, developing a good treatment plan can be an enormous challenge. One of the major difficulties in treatment planning is due to the presence of organs-at-risk (OARs), see Figure 1. An OAR is a healthy organ located close to the planning target volume (PTV or target). The dose of radiation must be constrained to avoid OARs because an overdose may lead to medical complications.

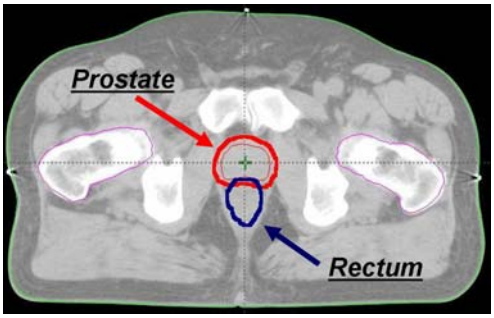

Figure 1. Two-dimensional organ geometry – prostate (target region) and rectum (OAR) are outlined in a 2D axial slice.

Conventionally, external-beam radiation treatments are delivered using a linear accelerator (LINAC) with a multi-leaf collimator (MLC or a beam shaper) housed in the head of the treatment unit (see Figure 2(a) and (b)). This device can rotate 360 degrees in one direction and make several stops to radiate *x-ray* beams. Various two-dimensional beam shapes can be constructed using a computer controlled MLC to conform the radiation beam to the shape of the tumor from any given angle. It is possible to determine the optimal amount of radiation for a fixed set of angles (beam angles or beam orientations) such that the final treatment plan can deliver a lethal dose of radiation to the target with minimum radiation exposure to the healthy organs. There are many different optimization models and methods for optimizing beam intensities in the literature. The most prominent distinction is between dose based and biological objective functions. The former usually minimizes deviations between desired and actual dose distributions whereas the latter model the radio-biological response of tissue and attempt to optimize the probability of successful treatment. For a survey see [39].

An advanced treatment planning approach, known as Intensity Modulated Radiation Therapy (IMRT), allows significant flexibility in delivering radiation from each beam angle [42]. IMRT was introduced as the state-of-the-art three-dimensional conformal radiation treatment (3DCRT) in the 1990s. In the last decade, techniques of IMRT have received significant attention among the medical community [11-13, 17, 18, 20, 23, 26-28]. In IMRT, an open radiation field is fractionated into hundreds of subfields called beamlets (or pencil beams; see Figure 2(c)). Each beamlet is assigned its own intensity called a beamlet weight. A matrix of beamlet weights from each beam orientation is often referred to as a fluence map. Obtaining an optimum setting of thousands of beamlet weights is nearly impossible if done manually, and therefore, specialized computer-aided optimization methods are often used.

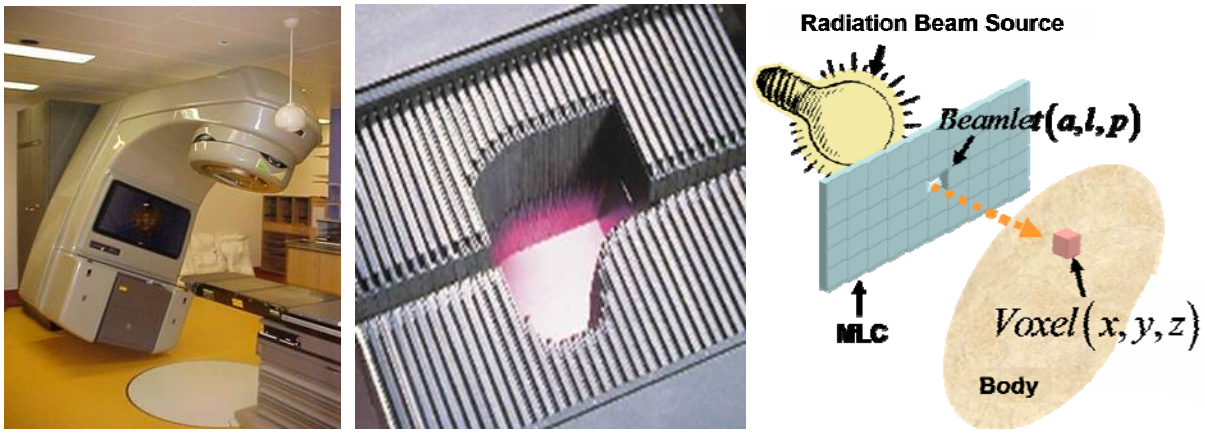

(a) A linear accelerator (b) A multi-leaf collimator (c) Beamlets (or Pencil beams)

Figure 2. An external beam delivery unit for IMRT.

Typically, the IMRT treatment plan is obtained by solving three sequential optimization problems: beam angle optimization (BAO), fluence map optimization (FMO), and beam segmentation (BS) [20]. In this paper, we present iterative solution methods from the BAO and the FMO problems in IMRT planning. We consider inverse treatment planning with a dose-based objective function. The BAO problem is to determine the positions of the gantry of a LINAC for which radiation is delivered [3, 4, 6-10]. We only consider coplanar beams for three-dimensional treatment planning in this paper.

Optimum beam orientations depend on a combination of factors such as anatomy, radiation tolerance, and the target's prescribed dose. Some theoretical considerations of optimizing beam orientations are discussed in [4, 41]. In many cited cases, the objective is to find a minimum number of beams that satisfy the treatment goals. However, we assume that the treatment planner knows how many beam angles will be used *a priori*. A number of researchers have reported different techniques for optimizing the beam orientations of an IMRT plan [7, 9, 15, 16, 21, 22, 24, 29-34, 36, 37, 40, 41]. Some

of the proposed objective functions for beam orientations are nonlinear and non-convex [4, 15, 41]. It is well known that such functions may have numerous local optimal solutions, which adds to the difficulty of obtaining a good solution. Therefore, choosing a proper solution method becomes critical in order to obtain a good solution.

One can perform the FMO on each of a large number of possible combinations of beam angles as a global search method. Stein et al. [41] apply an exhaustive search technique using a quadratic function for finding beam orientations. However, this involves a substantial amount of time to compare optimal dose distributions for all combinations and the problem becomes a large-scale combinatorial problem. Therefore, a BAO system based on an exhaustive search is considered to be too slow for a clinical setting.

As an alternative approach, guided random search techniques based on heuristic approaches such as simulated annealing [4, 6, 7, 33, 41] and genetic algorithms [3, 15, 25, 38] have been proposed. Simulated annealing is easy and flexible, but requires a large amount of computation time to obtain a good feasible solution. Genetic algorithms may not even converge to a good feasible solution unless sufficient randomness is given in the crossover and population selection.

Many other clever heuristics use *a priori* information about predetermined candidate beam angles to reduce the search space [7, 33, 35]. One of the most common approaches is a scoring method where scores are assigned to beam angles based on geometric and dosimetric information [7, 33]. Although scoring techniques can help reduce the computation time, such approximate schemes have the drawback that the inter-relationship between beam angles is ignored by calculating dosimetric parameters from a single incident beam angle plan. Therefore, the resulting solutions are likely to deviate from the global optimal solution. We explore an alternative approach to the scoring technique to optimize beam angles and the fluence maps in this paper.

The remainder of this paper is organized as follows. First, we introduce a mixed integer programming (MIP) formulation for finding the optimal set of beam angles and the corresponding fluence maps simultaneously in the next section. In Section 3, iterative solution methods are introduced to reduce the time needed to solve the MIP model. In Section 4, experiments using real patient cases demonstrate the computational advantage of the iterative methods for optimizing angles. Finally, we conclude this paper with a summary and our future work in Section 5.

2. Optimization Model Formulation

Our goal is to find an optimal set of beam angles and their corresponding beamlet weights. First, we describe a linear programming (LP) model that optimizes the beamlet weights. We assume that a set of beam angles are given as an input parameter. Therefore, our LP model only decides the optimal amount of radiation that each beamlet will deliver when the gantry is positioned at a given angle. This LP is easily

extended to a standard mixed integer programming (MIP) model to find an optimal set of beam angles, which is our second optimization model. In MIP, we assume that there are a finite number of candidate beam angles and the maximum number of beam angles for the treatment is given by the treatment planner.

We first define the input parameters as shown in Table 2.1. The following notations are self explanatory and are used throughout the paper.

Table 2.1. Definition of parameters.

Notation	Definition
A	a set of fixed beam angles, a is used to represent an individual angle, $a \in A$.
T	a set of voxels in planning target volume (PTV or target)
S	a set of voxels in organ-at-risk (OAR)
N	a set of voxels in normal structure
θ_L	cold spot control parameter on PTV
θ_U	hot spot control parameter on PTV
ϕ	hot spot control parameter on OAR
η	maximum number of treatment beam angles
L_T	lower reference bound on PTV
U_T	upper reference bound on PTV
$U_{\bar{N}}$	upper reference bound on normal structure
λ_t^+	penalty coefficient for hot spots on PTV
λ_t^-	penalty coefficient for cold spots on PTV
λ_s	penalty coefficient for hot spot on OAR
λ_n	penalty coefficient for normal structure
$d_{(x,y,z,a,l,p)}$	dose contribution from beamlet (a,l,p) to voxel (x,y,z) where $(x,y,z) \in T \bigcup S \bigcup N$, $a \in A$, $l \in \{1,2,\cdots,m\}$ and $p \in \{1,2,\cdots,n\}$

A *cold spot* is defined as a portion of an organ which receives a dose that is below its desired radiation dose level. A *hot spot* is a portion of an organ that receives a higher dose than its desired upper bound. Note that we use θ_L and θ_U to control cold spots and hot spots, respectively. The difference between θ_U and θ_L indicates how uniform the solution is. Ideally, we wish to achieve a treatment plan that has a zero gap. But in reality, achieving a zero gap is nearly impossible. Therefore, often a small gap is allowed in treatment planning.

Suppose that there are k organs-at-risk, S denotes the voxels in the OARs as a collection of k OARs $\left(S = S^1 \cup \cdots \cup S^k\right)$. Each voxel is identified by a three dimensional coordinate (x,y,z). The dose contribution is calculated via a Monte Carlo technique that simulates the track of a large number of

individual radiation particles. The full aperture is divided into rectangular subfields arranged in a $m \times n$ pattern, where m is the number of leaves and n represents the precision of an MLC, i.e. the number of stops of a leaf. Each beamlet is identified by the index pair (l, p), where $l = 1,2,\cdots,m$ and $p = 1,2,\cdots,n$. η is decided by the treatment planner depending on the tumor type. For example, eight beam angles are sufficient for head and neck cancer. For prostate cancer, five to seven beam angles are preferred [44].

2.1 Fluence Map Optimization Model

The primary variable is the beamlet weight $w_{a,l,p}$ that is defined over the $(l, p)^{th}$ beamlet delivered by an angle $a \in A$. A standard LP model is constructed to optimize the beamlet weights. The total dose $D_{(x,y,z)}$ that a voxel (x, y, z) receives is

$$D_{(x,y,z)} = \sum_{a,l,p} \left(w_{a,l,p} \right) \cdot d_{(x,y,z,a,l,p)}. \tag{2.1}$$

Based on this dose calculation, we impose upper and lower bounds on the target to avoid an undesirable dose distribution on the PTV, i.e., $L_T \le D_T \le U_T$. Most of the optimization models in the literature belong to a family of constrained optimization models such that an objective function is optimized while meeting these dose requirements.

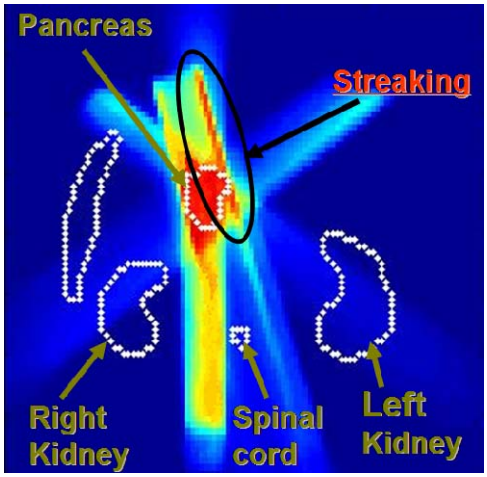

Figure 3. An example of streaking in IMRT planning.

One common concern in IMRT planning is the presence of “Streaking”. Streaking is a ray or rays of pencil beams that deliver an unusually high dose of radiation on the normal structure (See Figure 3), which is undesirable. There are different approaches to this problem either in the modeling stage or in the computational algorithm. We remedy streaking by imposing a strict upper bound on normal tissue that is

not close to the tumor. First, voxels on normal tissues are divided into two sets: one of which is in δ_{PTV} neighborhood N_{PTV}, i.e. $N_{PTV} = \left\{(x,y,z) \in N \mid \left\| PTV - (x,y,z) \right\|_2 \le \delta \right\}$ for some $\delta > 0$, and the other set is the complement of N_{PTV}, i.e. $\bar{N} = N \setminus N_{PTV}$.

Second, an upper bound $U_{\bar{N}}$ is imposed on $\bar{N}$, so that $D_{\bar{N}} \le U_{\bar{N}}$. The resulting LP model is

$$\begin{aligned} \min_{w} \quad & f(D) \\ s.t. \quad D_{(x,y,z)} &= \sum_{a \in A} \sum_{l=1}^{m} \sum_{p=1}^{n} \left(w_{a,l,p} \right) \cdot d_{(x,y,z,a,l,p)}, \qquad \forall (x,y,z) \in T \cup S \cup N \\ L_T &\le D_T \le U_T, \\ D_{\bar{N}} &\le U_{\bar{N}}, \\ 0 &\le w_{a,l,p} \le M_{a,l,p}, \qquad \forall a \in A,\ l = 1,2,\cdots,m,\ p = 1,2,\cdots,n \end{aligned} \tag{2.2}$$

where $M_{a,l,p}$ is an upper bound on $w_{a,l,p}$ (details about how to choose an appropriate value are discussed in Section 3). The objective function of the LP has three terms corresponding to the PTV, the OARs, and the normal tissue, and is written as follows:

$$\begin{aligned} f(D) = {} & \lambda_t^+ \left\| \left(D_T - \theta_U \cdot e_T \right)_+ \right\|_\infty + \lambda_t^- \left\| \left(\theta_L \cdot e_T - D_T \right)_+ \right\|_\infty \\ & + \frac{\lambda_s \left\| \left(D_S - \phi \cdot e_S \right)_+ \right\|_1}{|S|} + \frac{\lambda_n \left\| D_N \right\|_1}{|N|}. \end{aligned} \tag{2.3}$$

The notation $(\cdot)_+$ represents $\max\{\square, 0\}$. e_T and e_S are the vectors of ones, i.e. $e_T = 1^{|T|}$ and $e_S = 1^{|S|}$, respectively. The first two terms are based on the L_∞- norm that penalizes maximum violations for both hot spots and cold spots on the PTV. The third and the fourth terms penalize the average integral dose violation on OARs and normal structure, respectively. These penalty terms as well as the weights of each objective can be altered by the treatment planner.

2.2 Beam Angle Optimization Model

Model (2.2) is extended by introducing a new decision variable ψ_a for $a \in A$, that indicates whether the a^{th} angle is selected or not. We add another constraint to ensure that at most η angles are selected. Model (2.4) is the resulting MIP formulation for selecting optimal beam angles.

$$
\begin{aligned}
\min_{w,\psi} \quad & f(D) \\
s.t. \quad D_{(x,y,z)} &= \sum_{a\in A}\sum_{l=1}^{m}\sum_{p=1}^{n}\left(w_{a,l,p}\right)\cdot d_{(x,y,z,a,l,p)}, && (x,y,z)\in T\cup S\cup N \\
L_T &\le D_T \le U_T, \\
D_{\overline{N}} &\le U_{\overline{N}}, \\
\sum_{a\in A}\psi_a &\le \eta, \\
0 &\le w_{a,l,p} \le M_{a,l,p}\cdot\psi_a, && \forall a\in A,\ l=1,2,\cdots,m,\ p=1,2,\cdots,n \\
\psi_a &\in \{0,1\}, && \forall a\in A
\end{aligned}
\tag{2.4}
$$

Note that model (2.4) optimizes both the angles and the beamlet weights. Therefore, we consider (2.4) as a general formulation for solving the BAO and the FMO problems simultaneously.

Our model follows a standard linear optimization formulation. However, the real challenge lies in solving such problems because the input data (organ geometry and dose matrix) are often too large to handle. Storing the input data with a reasonable resolution in a clinical setting can easily take 5 to 10 GB of computer storage space. Due to the large amount of input data, solving the optimization models within a few hours becomes a serious challenge. We now discuss techniques that help to reduce the solution time for solving both models.

3. Iterative Solution Methods for Reducing Solution Time

Our primary focus in this section is to develop a few techniques that can help to drastically reduce the time to solve the MIP model (2.4). In general, there are more binary variables in the MIP, it takes longer to converge. Using this fact, we propose two new heuristic methods to reduce the number of candidate angles when solving the MIP. These heuristics are based on the MIP. We also explore some existing techniques in the literature to reduce the solution time [11, 12, 26-28]. First, we introduce iterative approaches that sequentially eliminate a subset of beam angles. Second, a method is presented to reduce the LP solution space by tightening bounds of beamlet weights.

3.1. Iterative Beam Angle Elimination (IBAE)

One of the obvious methods for solving the MIP model is the branch-and-bound (B&B) technique. Although such a method guarantees global optimality, solving the full MIP using B&B is not practically useful in the clinic due to its slow convergence. The LP model has many variables as well as many constraints. Therefore, it takes some time just to solve the LP problem. Now a feasible binary solution must meet the fourth constraint in (2.4). For example, if we want to choose 6 angles out of 36 candidate

beam angles, there are $C_6^{36} \cong 1,947,792$ combinations. Assuming that solving the LP (2.2) takes 2 minutes, solving the MIP model (2.4) may take 2706 days in the worst case.

The basic idea of our approach is to reduce the number of combinations in the beam angle optimization. We introduce an approach that takes two phases to determine a solution. The first phase is to find a promising set of beam angles by eliminating one insignificant angle per iteration. Here, insignificant beam angles are defined as beam angles that make relatively less contribution or no contribution to a better treatment plan compared to other beam angles. The second phase is to solve the model (2.4) using the reduced feasible set of binary variables obtained from the first phase. Since the second phase is trivial to understand, we will only explain two different implementations of the first phase.

A MIP Approach (IBAE – MIP)

Our first strategy is to eliminate one angle per iteration by repeatedly solving the MIP model (2.4) with decreasing values of η. We start with $\eta = |A| - 1,$ identify an insignificant angle that is eliminated to define a new candidate set A^i, reduce η by 1. This is repeated until η is the desired number of angles. A score is calculated based on the dosimetric information from the optimal solution at each iteration. Given an angle $a \in A^i$ at the i^{th} iteration, $i = 1, 2, \cdots, |A| - \eta,$ the average radiation dose $AvgDT_a^i$ for the PTV, and the average radiation dose $AvgDS_a^i$ for the OARs are calculated:

$$AvgDT_a^i = \frac{\sum_{(T)} \sum_{l,p} w_{a,l,p} \cdot d_{(T,a,l,p)}}{C_{(T,a)}}, \quad a \in A^i \tag{3.1}$$

$$AvgDS_a^i = \frac{\sum_{(S)} \sum_{l,p} w_{a,l,p} \cdot d_{(S,a,l,p)}}{C_{(S,a)}}, \quad a \in A^i \tag{3.2}$$

where $C_{(T,a)}$ and $C_{(S,a)}$ are number of voxels in the PTV and the OAR, respectively, that receive a positive radiation dose by the a^{th} beam angle. Then, we calculate the ratio that measures the dosimetric contribution to the PTV over the OARs:

$$Ratio^i = \frac{\sum_{a \in A^i} AvgDT_a^i}{\sum_{a \in A^i} AvgDS_a^i} \ . \tag{3.3}$$

A larger value of the ratio is preferred under the assumption that the radiation dose of each voxel is within an acceptable level specified for each organ. This process stops when a desired number of angles are obtained. Therefore, at most, $(|A| - \eta)$ iterations are required. One may adopt the final η angles for

the treatment. A more conservative approach is to stop the iteration when there are more than η angles at the end of the first phase, i.e., $\left|A^i\right| \le \eta + \alpha, \quad \alpha \in \mathbf{Z}_+$. In our approach, a set of promising beam angles A^{i^*} is defined as the one whose $Ratio^i$ is the highest over all $i = 1, 2, \cdots, \left|A\right| - k,$ where k is the cardinality of A^{i^*}, *i.e.*, $k = \eta + \alpha$. Finally, we move to the second phase to select η angles among A^{i^*} by solving (2.4). Figure 4 describes our iterative beam angle elimination algorithm. Note that η_0 is used as an alias to η in the optimization model, and is set to $\eta_0 = \eta + \alpha$.

Algorithm: Iterative Beam Angle Elimination - MIP

Initialize: $i = 1, \quad A^0 = A, \; k = \left|A^0\right|$;

while $\left(\left|A^{i-1}\right| > \eta_0\right)$

Step1: Solve (2.4) with $\eta = k - 1$.

Let $A^i = \left\{a \in A^{i-1} \mid \quad \psi_a > 0\right\}$ and $a^* = A^{i-1} \setminus A^i$;

Step2: Caculate $AvgDT_a^i$, $AvgDS_a^i$ and $Ratio^i$ where $a \in A^i$;

Step3: Store A^i and $Ratio^i$;

Step4: Fix $\psi_{a^*} = 0$;

Step5: Update index: $k = k$ -1, $i = i + 1$;

end

I = $i - 1$;

$i^* = \arg \max_{i \in \{1,2,\cdots,I\}} \left(Ratio^i\right)$;

Set $A = A^{i^*}$, and solve MIP (2.4) to determine optimal ψ and w;

Figure 4. An iterative beam angle elimination algorithm using B&B.

The computational complexity of IBAE-MIP is dominated by its linear programming (LP) solver for solving the LP sub-problems in Branch-and-Bound. In this approach, choosing 6 angles out of 36 in the first phase will require 30 MIP solves. Solving the MIP model in each iteration will require at most 36 binary decision variables in the worst case, i.e. at most 645 $\left(= C_{35}^{36} + C_{34}^{35} + \cdots + C_6^7\right)$ LP sub-problems. Therefore, IBAE-MIP is substantially faster than solving for the full MIP that chooses 6 angles out of 36. Note that IBAE-MIP eliminates one angle at each iteration and does not necessarily produce globally optimal solutions.

An LP Approach (IBAE – LP)

We introduce another beam selection criterion in this second implementation of the iterative approach. First, the LP model (2.2) is solved. Scores are calculated based on the dosimetric information from the optimal LP solution at the end of each iteration. We calculate the following basic measures. The quantity $uD(T)_a^i$ is the total amount of radiation that can be delivered to the tumor volume when one unit of delivery time is used for a given beam angle a at iteration i. $D(T)_a^i$, $D(S)_a^i$, and $D(N)_a^i$ are the projected total amount of radiation received by the PTV, the OAR, and the normal tissues from an angle a at the i^{th} iteration, respectively:

$$\begin{aligned} uD(T)_a^i &= \sum_{(x,y,z)\in T}\sum_{l,p} d_{(x,y,z,a,l,p)}, \qquad a \in A^i \\ D(\Omega)_a^i &= \sum_{(x,y,z)\in \Omega}\sum_{l,p} w_{a,l,p}\cdot d_{(x,y,z,a,l,p)}, \quad \Omega \in \{T,S,N\} \end{aligned} \tag{3.4}$$

After each iteration, three values are calculated per angle: a score for PTV, s_a^T, average *positive* dose scores s_a^S and s_a^N for OAR and the normal tissue, respectively:

$$s_a^T = D(T)_a^i \Big/ uD(T)_a^i, \quad s_a^S = D(S)_a^i \Big/ C_{(S,a)}, \text{ and } \quad s_a^N = D(N)_a^i \Big/ C_{(N,a)}. \tag{3.5}$$

Then, we calculate a linear combination of three function values as a merit score for each beam angle. Since we use different measures in the linear combination, each term is normalized to provide a fair judgment score:

$$Score(i,a) = \left(s_a^T \Big/ \sum_{a\in A^i} s_a^T \right) - \kappa_S \left(s_a^S \Big/ \sum_{a\in A^i} s_a^S \right) - \kappa_N \left(s_a^N \Big/ \sum_{a\in A^i} s_a^N \right), \quad 0 \le \kappa_S, \kappa_N \le 1. \tag{3.6}$$

The first term can be viewed as an *impact score* and the next two terms with weighting factors can be considered as an *avoidance score*. $Score(i,a)$ is desired to be as large as possible. An angle that has the lowest score is eliminated from the model (2.2). Therefore, there will be one less angle to consider in the model for the next iteration. This process continues until $|A^*| \le \eta + \alpha, \quad \alpha \in \mathbf{Z}_+$. Finally, we move to the second phase with $\eta + \alpha$ candidate angles for the MIP (2.4) to select η angles. Figure 5 describes the iterative beam angle elimination algorithm using LP.

Algorithm: Iterative Beam Angle Elimination - LP

$i = 1, \quad A^0 = A;$

while $\left(\left| A^i \right| > \eta_0 + \alpha \right)$

Step1: Solve IMRT LP (2.2);

Step2: Calculate uD_a^i, DT_a^i, DS_a^i, and DN_a^i for all $a \in A^i$;

Calculate $Score(i,a)$ for all $a \in A^i$ (3.6);

Step3: $a^* = \arg\min_{a \in A^i} Score(i,a)$;

Step4: Remove angle a^* from IMRT LP (2.2), *i.e.*, $A^i = A^{i-1} \setminus a^*$;

end

$A^* =$ angles at the end of this loop;

Set $A = A^*$, and solve IMRT MIP (2.4) to determine optimal ψ and w;

Figure 5. An iterative beam angle elimination algorithm using LP.

In this approach, choosing 6 angles out of 36 requires at most 30 LP solves, which is much easier than solving the full MIP model. One weakness of IBAE-LP is that it requires good values of the weighting factors, κ_S and κ_N.

A practical consideration for the stopping criterion in Phase I:

In practice, we add the secondary condition for choosing the promising beam angles: allow no more than a few extra angles in the optimization model in Phase II, say 4, $\alpha \le 4$. Since there are much less combinations for choosing an optimal subset of angles in the problem, solving (2.4) becomes tractable. The probability of getting a better solution for this iterative solution approach will be increased when there are more candidate angles in the optimization model (2.4). But if α is large, selecting η angles using the MIP model may still take long time in the second phase. This criterion applies to both IBAE-MIP and IBAE-LP.

3.2 Reducing the Feasible Region by Tightening Bounds on Beamlet Weights

The formulation (2.2) requires an upper bound $M_{a,l,p}$ on the beamlet weight $w_{a,l,p}$ for $a \in A$, $l \in \{1,2,\cdots,m\}$ and $p \in \{1,2,\cdots,n\}$. If $M_{a,l,p}$ is too small, the optimization problem can become infeasible or produce a local optimal solution. On the other hand, if the value is too large, the MIP model

may take a longer time to converge to a solution. A preprocessing step can be used to improve the bounds of the decision variables based on the input data so that the LP feasible region can be reduced. This can be done by calculating the maximum dose deliverable to the target for each beam angle when unit beam intensity is used [28]. The notation U_T denotes the maximum dose deliverable to voxels in the PTV. One of the constraints in model (2.2) holds core information to derive better bounds for the beamlet weights:

$$\sum_{a\in A}\sum_{l=1}^{m}\sum_{p=1}^{n}\left(w_{a,l,p}\right)\cdot d_{(x,y,z,a,l,p)} \le U_T. \tag{3.7}$$

For a given angle $a \in A$, and $l = 1,2,\cdots,m$, $p = 1,2,\cdots,n$, a relaxation for (3.7) for all PTV voxels $\forall\left(x,y,z\right)\in T$, can be expressed as

$$w_{a,l,p}\cdot d_{(x,y,z,a,l,p)} \quad \le \quad U_T. \tag{3.8}$$

The value on the left hand side represents dose level that a voxel $\left(x,y,z\right)$ can receive by a single pencil beam with the weight $w_{a,l,p}$. Therefore, an upper bound $M_{a,l,p}$ of beam weight $w_{a,l,p}$ can be calculated as follows:

$$M_{a,l,p} = \begin{cases} \dfrac{U_T}{\max\limits_{(x,y,z)\in T}\left(d_{(x,y,z,a,l,p)}\right)}, & \text{if } \max\limits_{(x,y,z)\in T}\left(d_{(x,y,z,a,l,p)}\right) > 0 \\ 0, & \text{otherwise.} \end{cases} \tag{3.9}$$

4. Numerical Experiments

4.1. Test Problem Setup

We test our methods on two data sets: prostate cancer and a pancreas tumor. The prostate cancer data contains two main organs of interest: prostate and rectum (see Figure 1). Using *4mm* precision of grids, the tumor region has 5246 voxels, the rectum has 1936 voxels, and the remaining healthy tissues have over 461,000 voxels on 38 CT slices. On the other hand, the pancreas tumor contains five organs of interest: pancreas, liver, left kidney, right kidney, and spinal cord (See Figure 7(b)). Their voxel counts are 1244, 50391, 9116, 5920, and 489, respectively on 90 CT slices.

Three possible scenarios are generated for 12, 24, and 36 candidate beam angles for the prostate tumor case. Our aim is to select six angles. For example, 12 beam angles are generated by equally dividing 360 degrees by 30 degrees as shown in Figure 7(a). Other sets of data (24 and 36 angles) are generated similarly. For the pancreatic tumor case, four angles will be selected for the treatment. Cases with 9, 12 and 36 candidate beam angles are considered.

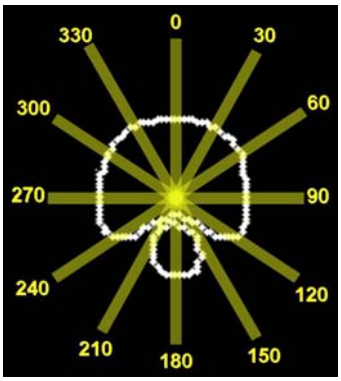

(a) Prostate cancer data: 12 equally spaced angles are depicted.

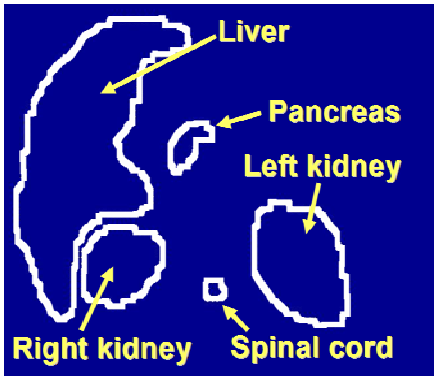

(b) Pancreas tumor and OARs

Figure 7. Organ geometry for prostate data (a) and pancreas data (b).

The specific optimization model considered in this section is the MIP model (2.4) in Section 2. We first assign values of the input parameters in the optimization model. Common parameters are $L_T = 0.94,\ U_{\bar{N}} = 0.75,\ \theta_U = 1.05,$ and $\theta_L = 0.96.$ Note that we normalized the prescribed dose on the PTV so that the value of 1 stands for the prescribed radiation dosage level on the tumor. There are problem specific parameters which include $\phi_{prostate} = 0.3$ and $\phi_{pancreas} = 0.2$ for the OARs, $U_T(prostate) = 1.15$ and $U_T(pancreas) = 1.07$ for the target, and $\eta_{prostate} = 6$ and $\eta_{pancreas} = 4$ for the desired number of treatment angles for the prostate and the pancreas data sets, respectively.

Typically, the values of weighting factors $\lambda_t^+, \lambda_t^-, \lambda_s,$ and λ_n are selected based on the planner's preference. In a trial-and-error approach, such values can be modified if the planner is not satisfied with the resulting solution. In our experiment, we assign a higher weight on the OAR than that of the PTV. This is because hard constraints are imposed on the PTV to meet the uniformity requirement. The optimization model will be solved to determine six significant angles for the prostate case and four angles for the pancreatic case along with their corresponding beamlet weights w.

Due to the massive amount of data in the case studies, we use the technique discussed in [29] to reduce the data points. This technique reduced the data size by up to 80% primarily on the normal tissue. However, all PTV and OAR voxels are included in the optimization model for the prostate case. One could sample data points on an OAR if it contains too many voxels such as the liver that is near the pancreas tumor. In our case study, a preprocessing step is performed to eliminate those voxels N^* in which it is not possible to receive a positive amount of radiation, i.e.,

$$N^* = \left\{ (x,y,z) \mid \sum_{a \in A} \sum_{l=1}^{m} \sum_{p=1}^{n} d_{(x,y,z,a,l,p)} \le \varepsilon, \quad \varepsilon > 0 \right\}.$$

This voxel elimination can substantially reduce the solution time without compromising the quality of a treatment plan. Note that if the value of ε is too large, it will corrupt the accuracy of the solution. In our study, ε is set to 10^{-6}. Furthermore, the upper bound of each beamlet weight $M_{a,l,p}$ is calculated by (3.9) to expedite the solution process.

All computations in this section were performed on a Pentium 4, 3.6 GHz PC running Linux. Optimization problems were modeled using GAMS (General Algebraic Modeling System) [45] modeling language. CPLEX 10.0 [19] was used to solve the LP model and the MIP model. The choice of LP solver can be crucial in reducing the solution time. We tried primal simplex, dual simplex, and interior point method. Both dual simplex and interior point method perform better than the primal simplex method. In our experiments, the interior point method slightly outperformed the dual simplex method. We would like to note that different CPLEX pricing schemes for the simplex methods may vary the solution speed. But we have not tried enough experiments to present in this paper. Therefore, we used the barrier method for solving the LP model and the branch-and-bound method [43] for solving the MIP model. The MIP solver is set to terminate when the dual gap falls below 3%.

4.2. Solution Quality and Performance Measure

In general, the solution quality of a treatment plan must meet at least three basic requirements to be practically useful: conformity, uniformity, and homogeneity [11, 12]. Researchers proposed several different methods to measure the quality of a treatment plan and include tumor control probability (TCP), normal tissue complication probabilities (NTCP), dose-volume histogram (DVH), and dose distribution (dose plot) [1]. In this paper, we will use DVH and three-dimensional radiation dose distribution to compare treatment quality and solution time to compare computational performance of each method.

Figure 8(a) shows a DVH example of a treatment plan based on the prostate tumor example discussed in the previous section. There are three lines: one for the PTV, one for the OAR and the third for the normal tissue. The point *p* can be interpreted as the point at which 50% of the entire tumor volume receives 100% of the prescribed dose level. Ideally, we aim to achieve a solution such that the DVH of the target region is perpendicular at relative dose 1.0 (i.e. all PTV voxels receive the exact amount of the prescribed dose) and the DVH of the OARs and the normal tissues is perpendicular at relative dose 0 (i.e. they receive no dose at all). On the other hand, a series of dose plots can provide positional information of the organs and the dose distribution to verify if a treatment plan meets the treatment goals. Figure

8(b).shows an axial slice of the dose distribution. This plot shows that the high dose radiation region conforms to the PTV while the OAR receives a very low radiation dose.

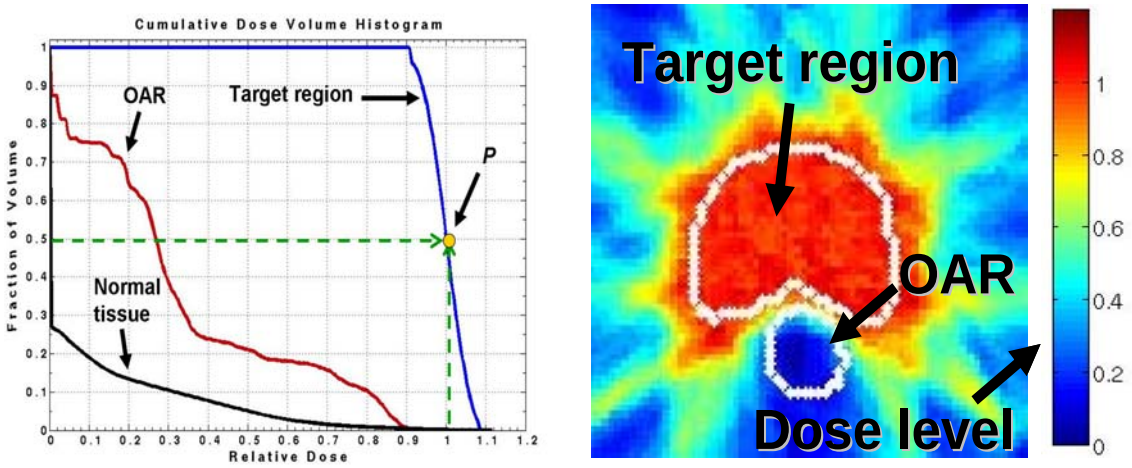

(a) An example of a DVH (b) An example of a dose plot

Figure 8. Evaluation tool for treatment plans.

4.3. Results

Three sets of experiments are designed to compare computational performance among different strategies for optimizing beam angles and their fluence maps as shown in Table 4.1. First, the MIP model (2.4) is solved to benchmark solution quality for other methods. Then two iterative beam angle elimination algorithms are applied as described in Section 3.1.

Table 4.1. Three techniques are tested to compare the performance.

Method	Procedure to obtain a solution
MIP	• The MIP model (2.4) is solved to obtain optimal angles and the corresponding fluence maps simultaneously.
IBAE – MIP	• Iterative Beam Angle Elimination algorithm – MIP approach, $\alpha = 2$
IBAE – LP	• Iterative Beam Angle Elimination algorithm – LP approach, $\alpha = 2$

Table 4.2 shows the optimal angles obtained from the MIP and final angles from two heuristic methods when 12 candidate angles are available for the prostate cancer data. It is interesting to see that IBAE-LP was able to find a solution that is close to the globally optimal (MIP) solution with a fraction of

computation time, i.e., 92% computation time reduction compared to the full MIP. In fact, the only different angle (angle 180) turned out to be an opposite angle to angle 0.

Table 4.2. Optimal beam angles obtained from 12 candidate angles (Prostate).

	Final beam angles	Objective value	Time (min)	Reduction
MIP	0°, 90°, 120°, 150°, 210°, 240°	0.270	313.2	-
IBAE-MIP	30°, 90°, 120°, 150°, 180°, 240°	0.274	89.3	71%
IBAE-LP	90°, 120°, 150°, 180°, 210°, 240°	0.275	25.3	92%

The IBAE-MIP solution missed two angles compared to the global solution while it took about 3.6 times longer than the IBAE-LP to converge. Figure 9 shows a trend of the ratio in IBAE-MIP over five iterations. Since $Ratio^4$, i.e., $i^* = 4$, has the highest value and the number of angles is within $[\eta, \quad \eta + \alpha] = [6, \quad 8]$, the first phase will have 8 angles in the promising set obtained at the fourth iteration, i.e., $A^4 = \{30, 60, 90, 120, 150, 180, 240, 270\}$. Now, we solve the MIP (2.4) to select the final 6 beam angles among 8 in A^4. Note that it was not necessary to perform the fifth iteration because the value of α was set to 2.

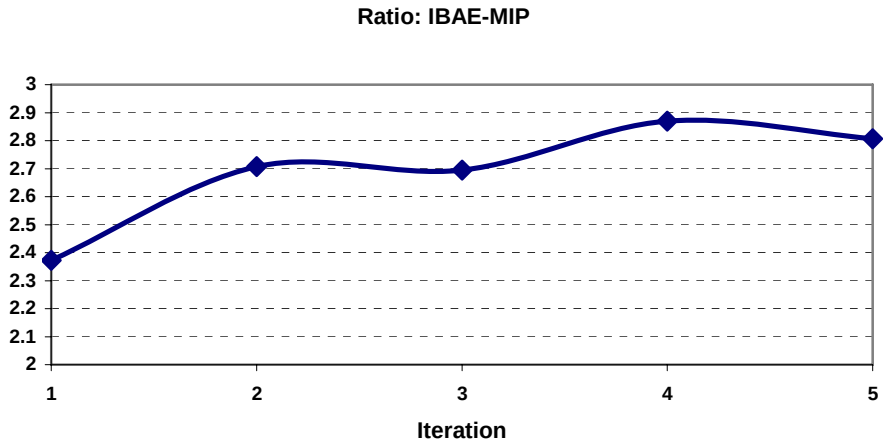

Figure 9. Ratio of each iteration in IBAE-MIP

Figure 10 shows the DVH lines on the PTV and the normal tissues for three methods we tried. When we draw a vertical line at relative dose 0.3 ($\phi = 0.3$ in the optimization model), OAR lines of the full MIP and two iterative methods are almost identical. DVH lines of PTV and Normal are also identical. Figure 11 compares the dose distribution of the three different plans and supports that the three treatment

plans are almost identical. This indicates that all three treatment planning methods can produce equally good plans, especially, the iterative methods are as good as the full MIP model.

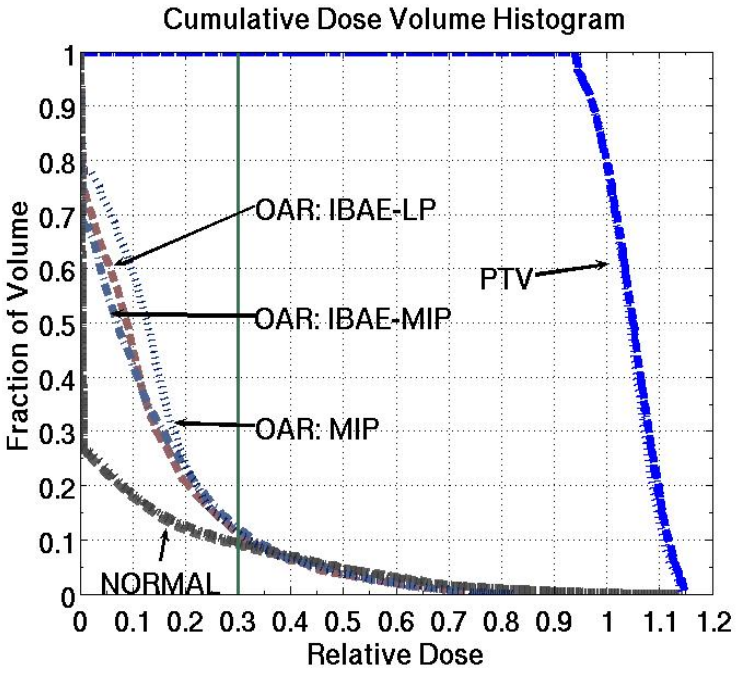

Figure 10. Comparison of Dose Volume Histograms: IBAE-LP, IBAE-MIP, and MIP (Prostate).

At first, the DVH lines of the two heuristics appear to be better than that of the full MIP on the left side of the vertical line at relative dose 0.3. But this can happen because the optimization model does not penalize any voxels that receive less 30% of the prescribed radiation dose. Therefore, mathematically, there is no difference among these methods on that region. However, there is a difference in hot spots as can be seen in Table 4.2. The objective value of the full MIP is smaller than those of the two heuristic methods.

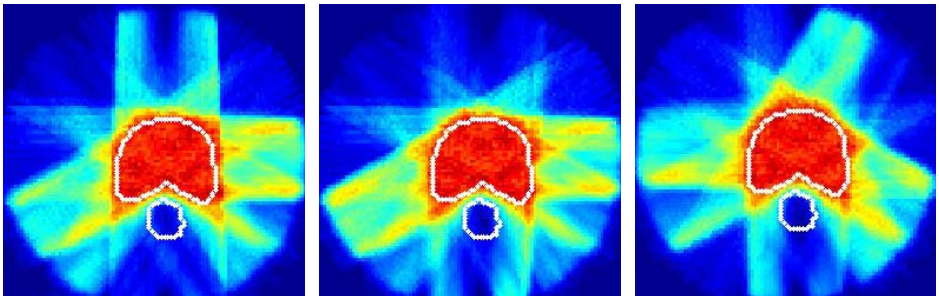

(a) MIP (b) IBAE – LP (c) IBAE – MIP

Figure 11. Dose distribution plots for different angle optimization techniques.

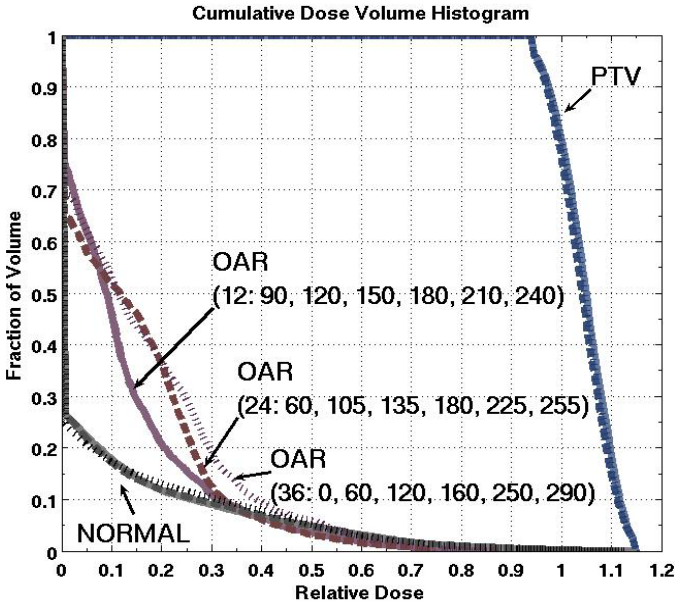

Figure 12. Comparison of Dose Volume Histograms for 12, 24, and 36 candidate angle cases (Prostate).

In general, adding more candidate angles will improve the solution quality. However, this logic may not apply to our iterative methods. Figure 12 shows DVH lines for three different candidate angle configurations for prostate cancer data. The IBAE – LP method is used to compare the solution quality when 12, 24, and 36 candidate angles are used in the problem. The lines of DVH look identical among all methods on the PTV and the normal tissues. But, the DVH line gets worse as there are more candidate angles. This trend is not surprising because the iterative LP method, a heuristic approach, may add more errors as there are more iterations involved. Therefore, adding more candidate angles may not guarantee a better solution when the iterative methods are applied. However, such an iterative method can be beneficial because a good treatment plan can be obtained from a small number, say 12, of candidate angles.

The performance of the iterative methods was superb when they were applied to the pancreas tumor data. Table 4.3 shows the results when three different methods are applied to select optimal angles from 12 candidate angles. Both of the iterative methods produced the same solution that is near the global optimal solution. The iterative MIP (IBAE-MIP) reduced the computation time by 61% while the iterative LP reduced the time by 77%.

Table 4.3. Optimal beam angles obtained from 12 candidate angles (Pancreas).

	Beam angles	Objective value	Time (min)	Reduction
MIP	90°, 120°, 180°, 240°	0.110	60.92	-
IBAE-MIP	90°, 120°, 180°, 210°	0.117	23.90	61%
IBAE-LP	90°, 120°, 180°, 210°	0.117	13.80	77%

Finally, we show the computation time for different angle configurations for both the prostate and the pancreas data sets in Table 4.4. Figure 13 shows the trend of computation time as the candidate angles increases. The MIP model solved all three cases of the pancreas data within 14 hours. But the model failed to solve the prostate data within 10 days for both 24 and 36 candidate angle cases. We note that the dual gap for the 36 angle case showed 64% when the branch-and-bound algorithm was manually terminated at the 10^{th} day.

Table 4.4. Computation time comparison (minute)

	Prostate			Pancreas		
	Number of candidate angles			Number of candidate angles		
	12	24	36	9	12	36
MIP	313.20	---	---	30.90	60.92	833.62
IBAE-MIP	47.20	300.78	720.0	21.87	23.9	65.97
IBAE-LP	25.28	46.16	82.2	13.8	13.8	63.76

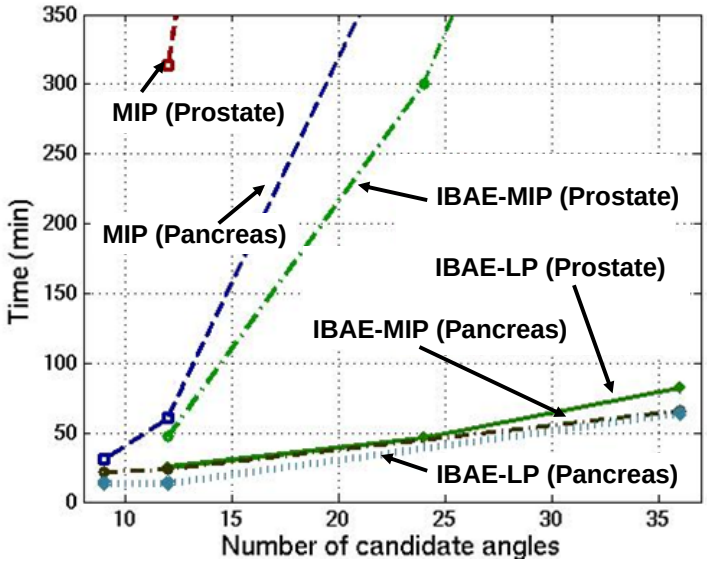

Figure 13. Computational time comparison.

Optimal fluence maps are byproducts of optimizing the angles when IBAE-MIP and IBAE-LP are used. Therefore, no extra effort is necessary to get the optimal fluence. Figure 14 shows the DVH plots of the final solution obtained from IBAE-MIP and IBAE-LP whose optimal angles are discussed in Table 4.3. First of all, the tumor region receives a relative dose ranging from 95% to 105% of the prescribed dose. The entire spinal cord, which is a serial organ, is well protected by receiving less than 24% of the target prescribed dose level. On the other hand, more than 99% of the liver, a parallel organ, receives less than 30% of the target prescribed dose level.

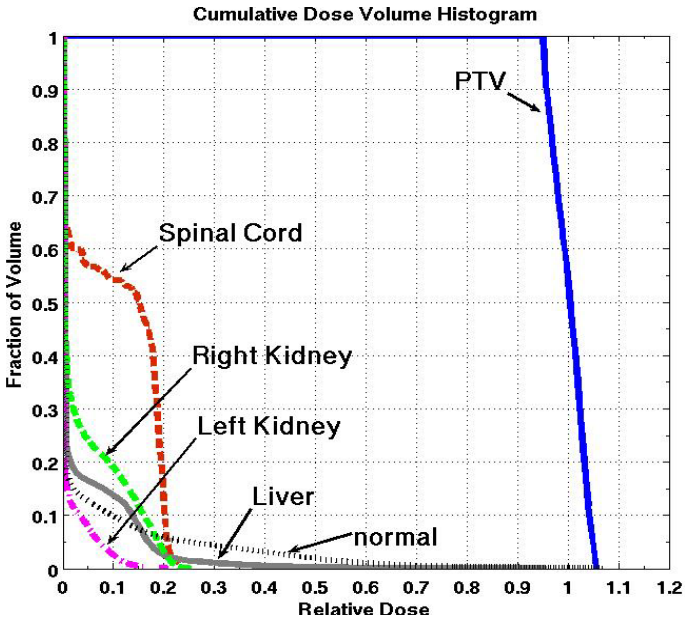

Figure 14. Dose Volume Histogram of the solution of the iterative MIP and the iterative LP (pancreas).

5. Conclusion and Future Work

We have presented various techniques for solving the beam angle and the fluence map optimization problems simultaneously. A mixed integer programming (MIP) model and a linear programming (LP) model are presented as the underlying optimization models. The MIP model is solved using the branch-and-bound technique while the LP model is solved using the interior point method. Due to the large amount of data in the optimization models, solving the optimization problems can take weeks of computation time. Therefore, we introduced iterative angle optimization approaches to expedite the solution time. Two iterative beam angle elimination algorithms are developed for selecting optimal angles. The first approach solves the MIP model iteratively by eliminating one insignificant angle at a time. The second approach uses the LP model to generate scores for angles and eliminates one angle whose score is the smallest in each iteration. This process continues until there are $\eta + \alpha$ angles in the problem. Then the

MIP model is applied to select the best η angles out of $\eta + \alpha$. Voxel reduction and reducing the LP solution space are also implemented to help expedite the solution time.

Computational experiments are made to compare, among three different approaches, the solution time and the treatment quality using two case examples: prostate tumor and pancreas tumor. First, the MIP model was solved using the branch-and-bound method and the results were used to benchmark the solution quality of the other methods discussed. The iterative LP approach seems to perform very well in both tumor cases in the different angle configurations we tried. In fact, the solution quality of the iterative methods was close to the global optimal solutions for both tumor cases. We also made significant progress in reducing the solution time. The iterative LP was able to solve all six problem instances within 1 ½ hours.

A few improvements are required for our optimization model to be practically useful. First, further investigation is needed to design robust stopping criteria for the iterative beam angle elimination algorithms. Second, more experiments are needed to fine-tune our solution techniques. Third, more robust score functions can also help correctly evaluate optimal beam angles when the iterative angle elimination algorithms are used. Finally, both of the iterative algorithms can be used as starting solution generation methods for other optimization approaches. These items comprise the list of our future work.

Acknowledgement. This work was supported in part by University of Houston GEAR Grant #91063

References

[1] Alber, M., F. Nusslin. 1999. An objective function for radiation treatment optimization based on local biological measures. *Phys. in Medicine and Biol.* 44 479-493.

[2] American Cancer Society. Cancer Facts &Figures 2005. *http://www.cancer.org/downloads/STT/CAFF2005f4PWSecured.pdf.*

[3] Bevilacqua, V., G. Mastronardi, G. Piscopo. 2003. Full beam configuration for coplanar radiotherapy inverse planning: A genetic algorithm-based framework. *Proc. of Artificial intelligence and applications.*

[4] Bortfeld, T., W. Schlegel. 1993. Optimization of beam orientations in radiation therapy: some theoretical considerations. *Phys. in Medicine and Biol.* 38 291-304.

[5] Brook. A., D. Kendrick, A. Meeraus, and R. Raman, GAMS: A User's Guide, GAMS Development Corporation: http://www.gams.com/, 2002.

[6] Djajaputra, D., Q. Wu, Y. Wu, R. Mohan. 2003. Algorithm and performance of a clinical IMRT beam-angle optimization system. *Phys. in Medicine and Biol.* 48:3191-212.

[7] D'Souza, W. D., R. R. Meyer, L. Shi. 2004. Selection of beam orientations in intensity-modulated radiation therapy using single-beam indices and integer programming. *Phys. in Medicine and Biol*. 49:3465-81.

[8] Ehrgott, M., M. Burjony. 2001. Radiation therapy planning by multicriteria optimization. *Proc. of the 36th Annual Conf. of the Oper. Res. Soc. of New Zealand.* 27:244–253.

[9] Ehrgott, M., R. Johnston. 2003. Optimisation of beam directions in intensity modulated radiation therapy planning. *OR Spectrum.* 25:251–264.

[10] Ezzell, G. A. 1996. Genetic and geometric optimization of three-dimensional radiation therapy treatment planning. *Medical Phys.* 23:293-305.

[11] Ferris, M. C., J. Lim, D. M. Shepard. 2003a. Optimization approaches for treatment planning on a Gamma Knife. *SIAM J. on Optim.* 13:921–937.

[12] Ferris, M. C., J. Lim, D. M. Shepard. 2003b. Radiosurgery treatment planning via nonlinear programming. *Annals of Operations Research.* 119:247–260.

[13] Ferris, M. C., R. R. Meyer, W. D'Souza. Radiation treatment planning: Mixed integer programming formulations and approaches. H. P. Williams, G. Appa, L. Pitsoulis, eds., Handbook on Modelling for Discrete Optim., Kluwer Academic Publishers, Boston, MA, 2005.

[14] Gokhale, P., E. M. A. Hussein, and N. Kulkarni. 1994. Determination of beam orientation in radiotherapy planning. *Medical Phys.* 21(3):393–400.

[15] Haas, O. C. L., K. J. Burnham, J. A. Mills. 1998. Optimization of beam orientation in radiotherapy using planar geometry. *Phys. in Medicine and Biol.* 43:2179-93.

[16] Hamacher, H. W., K.-H. K¨ufer. 2002. Inverse radiation therapy planning — a multiple objective optimization approach. *Discrete Appl. Math.* 118:145–161.

[17] Holder, A. 2003. Designing radiotherapy plans with elastic constraints and interior point methods. *Health Care and Management Science* 6:5–16.

[18] Holder, A. 2004. Radiotherapy treatment design and linear programming. M.L. Brandeau, F. Sainfort, W.P. Pierskalla, eds., Oper. Res. and Health Care: A Handbook of Methods and Applications. *Kluwer Academic Publishers, Boston*, MA 741–774.

[19] ILOG CPLEX 10.0, http://www.ilog.com.

[20] Intensity Modulated Radiation Therapy Collaborative Working Group. 2001. Intensity modulated radiotherapy: current status and issues of interest. *Internat. J. of Radiation Oncology: Biol., phys.*51:880-914.

[21] Johnston, L. A. 2002. Optimisation of irradiation directions in IMRT treatment. *Proc. Of the 37th Annual Conf. of the Oper. Res. Soc. Of New Zealand.*

[22] Langer, M., R. Brown, M. Urie, J. Leong, M. Stracher, J. Shapiro.1990. Large scale optimization of beam weights under dose-volume restrictions. *Internat. J. of Radiation Oncology: Biol., phys.*18:887–893.

[23] Lee, E. K., T. Fox, I. Crocker. 2000. Optimization of radiosurgery treatment planning via mixed integer programming. *Medical Phys.* 27:995–1004.

[24] Lee, E. K., T. Fox, I. Crocker. 2003. Integer programming applied to intensity-modulated radiation therapy treatment planning. *Annals of Operations Research.* 119:165–181.

[25] Li, Y., J. Yao, D. Yao. 2004. Automatic beam angle selection in IMRT planning using genetic algorithm. *Phys. in Medicine and Biol.* 49:1915-32.

[26] Lim, J. 2002. Optimization in radiation treatment planning. *Ph.D. dissertation*, *University of Wisconsin-Madison, Madison, Wisconsin.*

[27] Lim, G. J, M. C. Ferris, and D. M. Shepard. 2004. Optimization tools for radiation treatment planning in matlab. In M.L. Brandeau, F. Saintfort, and W.P. Pierskalla, editors, Operations Research And Health Care: A Handbook of Methods and Applications, pages 775–806. *Kluwer Academic Publishers, Boston.*

[28] Lim, G. J, M. C. Ferris, S. J. Wright, D. M. Shepard, and M. A. Earl. 2006. An optimization framework for conformal radiation treatment planning. to appear, *INFORMS Journal On Computing.*

[29] Meedt, G., M. Alber, F. Nusslin. 2003. Non-coplanar beam direction optimization for intensity-modulated radiotherapy. *Phys. in Medicine and Biol.* 48:2999-3019.

[30] Preciado-Walters, F., R. Rardin, M. Langer, and V. Thai. 2004. A coupled column generation, mixed-integer approach to optimal planning of intensity modulated radiation therapy for cancer. Mathmatical Programming, 101:319-338.

[31] Price, R. A., G. E. Hanks, S. W. McNeeley, E. M. Horwitz, W. H. Pinover. 2002. Advantages of using noncoplanar vs. axial beam arrangements treating prostate cancer with intensity-modulated radiation therapy and the step-and-shoot delivery method. *Internat. J. of Radiation Oncology: Biol., phys.* 53:236-43.

[32] Pugachev, A., J. G. Li, A. L. Boyer, S. L. Hancock, Q. T. Le, S. S. Donaldson, L. Xing. 2001. Role of beam orientation optimization in intensity-modulated radiation therapy. *Internat. J. of Radiation Oncology: Biol., phys.*50:551-60.

[33] Pugachev, A., X. Lei. 2002. Incorporating prior knowledge into beam orientation optimization in IMRT. *Internat. J. of Radiation Oncology: Biol., phys.*54:1565-74.

[34] Rowbottom, C. G., V.S. Khoo, and S. Webb. 2001. Simultaneous optimization of beam orientations and beam weights in conformal radiotherapy. *Medical Phys.* 28(8):1696–1702.

[35] Rowbottom, C. G., S. Webb, M. Oldham. 1998. Improvements in prostate radiotherapy from the customization of beam directions. *Medical Phys.* 25:1171-9.

[36] Rowbottom, C. G., S. Webb, M. Oldham. 1999. Beam-orientation customization using an artificial neural network. *Phys. in Medicine and Biol.* 44:2251-2262.

[37] Schreibmann, E., L. Xing. 2004a. Feasibility study of beam orientation class-solutions for prostate IMRT. *Medical Phys*. 31:2863-70.

[38] Schreibmann, E., M. Lahanas, L. Xing, D. Baltas. 2004b. Multi-objective evolutionary optimization of the number of beams, their orientations and weights for intensity modulated radiation therapy. *Phys. in Medicine and Biol.* 49 747-770.

[39] Shepard, D.M., Ferris, M.C., Olivera, G., and Mackie, T.R., Optimizing the delivery of radiation to cancer patients, *SIAM Review,* 41:721-744, 1999.

[40] Soderstrom, S., A. Gustafsson, and A. Brahme. 1995. Few-field radiation-therapy optimization in the phase-space of complication-free tumor central. *International Journal of imaging systems and technology.* 6(1):91–103.

[41] Stein, J., R. Mohan, X. H. Wang, T. Bortfeld, Q. Wu, K. Preiser, C. C. Ling, W. Schlegel. 1997. Number and orientations for beams in intensity-modulated radiation treatments. *Medical Phys.* 24:149-160.

[42] Webb, S. 2001. Intensity-modulated radiation therapy. C. G. Orton, J. A. E. Spaan, J. G. Webster, eds. *Institute of physics, Series in medical physics, IOP Publishing Ltd*.

[43] Wolsey, L. A. 1998. Integer programming. Wiley-Interscience Series in Discrete Mathematics and Optimization, *John Wiley & Sons, Inc*.

[44] Xia, P. 2005. Fundamental Issues in IMRT treatment planning, *AAPM 47 the Annual meeting, course MO-B-T-6E*.